

Magneto-elastic tuning of ferroelectricity within a magnetoelectric nanowire

Stephanie H. Johnson,¹ Peter Finkel,² Oren D. Leaffer,¹ Stephen S. Nonnenmann,¹ Konrad Busmann,³ and Jonathan E. Spanier^{1,a)}

¹Department of Materials Science and Engineering, Drexel University, Philadelphia, Pennsylvania 19104, USA

²U.S. Naval Undersea Warfare Center, Code 1512, Newport, Rhode Island 02841, USA

³U.S. Naval Research Laboratory, Code 6360, Washington DC 20375, USA

(Received 8 April 2011; accepted 7 October 2011; published online 31 October 2011)

Nanowires each consisting of a magnetostrictive Co core and a $\text{PbZr}_{0.52}\text{Ti}_{0.48}\text{O}_3$ or BiFeO_3 ferroelectric oxide shell exhibit a magnetic field-tunable piezoelectric response and ferroelectric coercivity owing to magneto-elastic coupling through the interfacial core-shell boundary. The observed magneto-elastic tuning of the ferroelectric switching is analyzed using a renormalized Landau-Ginzburg stiffness in which a magnetic field-tunable stress concentration is incorporated. These results provide insight into the design of integrated functional devices and magnetoelectric sensors. © 2011 American Institute of Physics. [doi:10.1063/1.3657152]

Understanding of the strength and size scalability of coupling of physical properties in composite solids, namely those associated with correlated magnetic and dipolar order and the roles of shape and arrangement of the constituent phases, is central to realizing high-performance magneto-electrics (MEs) and their applications. A wealth of evolving knowledge of the effects of chemistry, of magnetic and dipolar order, of microstructure, and of sample size and geometry on intrinsic and extrinsic ME properties of solids informs the materials selection and design of ME devices.^{1–5} In the design of extrinsic multiferroics, however, the potential benefit of maximizing interfacial area using nanostructured constituent ferromagnetic (FM) and ferroelectric (FE) components on ME properties is typically offset by a suppression of ferroic and piezoelectric properties in nanostructured solids.

The introduction of extreme curvature in an ultra-thin FE film⁶ enables an enhanced electrostrictive coupling of non-uniform stress with FE polarization, permitting a finite curvature-enhanced increase in the FE properties compared with planar films of identical composition and thickness.⁷ We report here on a highly tunable ME coupling within individual multiferroic nanowires (NWs) measured by the direct ME effect. Core-shell NWs each comprising a FM metal core surrounded by a FE oxide shell exhibit an enhanced and tunable coupling of static magnetic-field with piezoelectric response and FE switching properties. The tunable electro-mechanical response, which is due to magneto-elastic modification of the interfacial mechanical boundary condition, is enhanced by the large surface-to-volume ratio in the co-axial NWs, by the extreme curvature of the FE shell and by the magnetic shape anisotropy within the NW core.

NWs of 200 nm in diameter each consisting of a ~180-nm diameter FM metal (Co) core and a ~10-nm thick FE oxide (either $\text{PbZr}_{0.52}\text{Ti}_{0.48}\text{TiO}_3$ (PZT) or BiFeO_3) shell were produced using a template assisted core-shell growth method.⁶ Briefly, sol-gel precursors comprising $\text{Bi}(\text{NO}_3)_3 \cdot 5\text{H}_2\text{O}$ and $\text{Fe}(\text{NO}_3)_3 \cdot 9\text{H}_2\text{O}$ with a 1:1 molar ratio are

mixed with 100 ml ethylene glycol and stirred at 80 °C for 1 h. The precursor is then dispensed onto anodic Al_2O_3 templates possessing (~200-nm diameter pores), and the templates were subjected to an annealing sequence in atmosphere: 1 h @ 100 °C, 2 h @ 400 °C, and finally 4 h @ 650 °C, forming perovskite oxide cylindrical shells. This was followed by a potentiostatic (5 V, working-to-Pt counter electrode) cathodic reduction of $\text{CoSO}_4 \cdot 7\text{H}_2\text{O}$ mixed with $\text{B}(\text{OH})_3$ producing Co NWs (Ref. 8) within the oxide perovskite shells. Templates were dissolved using 6 M NaOH. X-ray powder diffraction of identically prepared and annealed nanotubes in templates was collected to validate that the product is pure-phase BiFeO_3 and $\text{PbZr}_{0.52}\text{Ti}_{0.48}\text{O}_3$.⁶

NWs were dispersed onto Si(100) substrates possessing a 200-nm thermally grown SiO_2 film. Following electron beam lithographic patterning to define areas for electrical contact in a region near the end of each NW, the oxide shells were selectively wet-etched for 3 min using a solution consisting of 75 ml H_2O , 40 ml 10% NH_4Cl , 6 ml HCl , 6 ml HNO_3 , 6 ml CH_3COOH , 1 ml of 6:1 buffered HF (8 g NH_4F and 20 ml H_2O), and 2 g EDTA stirred at 300 rpm for 15 min.⁹ Thermal evaporation of Cr(5 nm)/Au(200 nm) was used to electrically contact the metal core of each core-shell NW (Fig. 1). For comparison with a planar bi-layer thin film, a ~100-nm thick Co film was deposited using electron-beam evaporation on a platinized Si(100) substrate, followed by deposition of a ~300-nm thick layer of BiFeO_3 film using the sol-gel route described above.

Ferroelectric switching and piezoelectric responses were measured using an experimental configuration described elsewhere.⁷ In addition, a static magnetic field ($0 < H < 2$ kOe) was applied perpendicular and alternately, parallel, to the axis of each NW studied and within the plane of the bi-layer thin-film substrate. For $H = 0$, the BiFeO_3 and PZT shells exhibit FE switching, with coercive field comparable to values reported for PZT nanotubes.^{6,7} However, the application of an H -field perpendicular to the axis of the NW during collection of the variation of piezoresponse amplitude (η) with voltage results in an approximate doubling in d_{33} ($\equiv \delta\eta/\delta V$) over the range $0 < H < 2$ kOe (Figs. 2(a) and

^{a)}Electronic mail: spanier@drexel.edu.

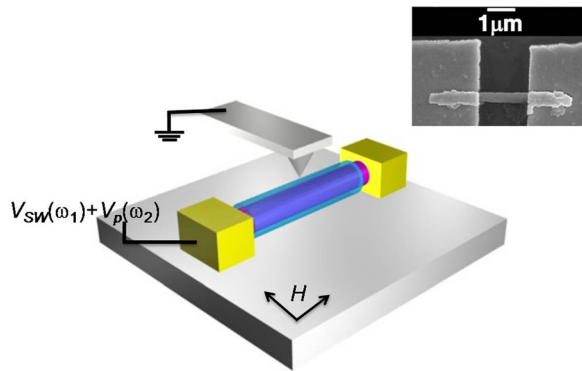


FIG. 1. (Color online) Schematic illustration of the magnetolectric core-shell NW, electrode configuration, and probing geometry. H is applied along the axis of the NW (z) and alternately $H \perp z$ and in the plane of the substrate while a waveform comprising switching (V_{SW}) and probing (V_P) components is applied directly to the electrically contacted Co core. *Inset*: scanning electron micrograph of an electrically contacted Co-core BiFeO₃-shell NW.

2(b)), in stark contrast to the decrease over the same range for the thin-film Co/BiFeO₃ multilayer structure (Fig. 2(c)). A summary of the data for the variation in d_{33} with H for each case is shown in Fig. 3(a). The application of H is also seen to alter the FE switching properties; the hysteresis loop width ΔV (defined here as the voltage difference between the two minima in the piezoresponse amplitude, identified for each value of H) increases from ~ 0.4 V to ~ 1.1 V for $0 < H < 2$ kOe (Fig. 2(d)). Notably, no systematic variation in the piezoelectric response with magnetic field was observed in NWs consisting of non-FM (Au) metal NW cores, indicating the key role of the FM cores. In addition, application of the H field *parallel* to the long axis (z) of a PZT NW also resulted in no discernable systematic variation in the piezoelectric response (Fig. 3(a)).

Ferromagnetic NWs possessing a diameter comparable to magnetic thin-film thickness and nanoparticle diameter feature an aspect ratio-dependent magnetic shape anisotropy in which preferred orientation of magnetization aligns along the long axis of the wire.^{3,10,11} We propose that the magnetic shape anisotropy causes the magnetization to lie preferentially along z so that application of $H \perp z$ results in a re-orientation of the magnetic moments, resulting in a large

magnetostriction owing to the re-orientation.¹⁰ Magnetostrictive coupling contributes a H -field dependent stress at the interface of the Co-core and FE oxide shell. While a direct analysis of the coupling of local magnetic and dipolar orientation with structure is not feasible due to the nanocrystalline structure of the core and shell,⁶ an altered (interfacial) mechanical boundary condition can account for the field-dependent piezoelectric response and FE coercivity.

Following this line of argument, we contend that application of $H \parallel z$ leaves the orientation of a majority of the magnetic moments unchanged and principally along z . However, the variation in the amplitude of electromechanical response from the BiFeO₃ and PZT shells for $H \perp z$ is seen to scale as $\sim H^2$. Fitting the measured response with $d_{33}(H) = c_0 + cH^2$ yields $c_{0,\text{BiFeO}_3} = 20.9 \pm 6.4$ pm/V, $c_{0,\text{PZT}} = 28.5 \pm 1.16$ pm/V, and $c_{\text{BiFeO}_3} = 5.67 \times 10^{-6} \pm 2.55 \times 10^{-6}$ pm V⁻¹ Oe⁻², and $c_{\text{PZT}} = 7.62 \times 10^{-6} \pm 4.65 \times 10^{-7}$ pm V⁻¹ Oe⁻², respectively. This quadratic dependence is understood in terms of fundamental domain wall motion theory stating that in the low-field limit the magnetostriction is $\sim H^2$.¹⁰ Further, $\delta d_{33}/\delta H > 0$ at $H = 2$ kOe, the maximum controllable field in our experimental apparatus; we expect saturation at sufficiently larger values of H . Differences in fitted values of c are not large when considering the experimental scatter in the measurement of d_{33} for each value of H and the error in fitting c , suggesting that the quadratic coupling of H with piezoelectric response, even in the intrinsic multiferroic BiFeO₃, is dominated by the magneto-elastic coupling of the two-component ME nanostructure.

Application of $H \perp z$ is also seen to modify the FE switching in Co-BiFeO₃ NWs. We note that FE hysteresis loop width ΔV varies much more strongly at larger H (~ 1.5 – 2.0 kOe), particularly given the small scatter (Fig. 3(b)); a similar effect was also observed for Co-PZT NWs (not shown). Fitting the data shown in the Fig. 3(b) using a power law produces much better agreement with data as compared with a quadratic: $\Delta V = \Delta V_0 + kH^\alpha$, with $\Delta V_0 = 0.407 \pm 0.027$ V and $\alpha = 5.09 \pm 0.011$ ($k \equiv 1 \times 10^{-17}$).

This tuning of FE coercivity can be understood in terms of a magnetoelastic modulation of the compressive radial stress σ_{rr} at the interface of the magnetostrictive core and FE shell. Following Ref. 7, we apply the Landau-Ginzburg (LG)

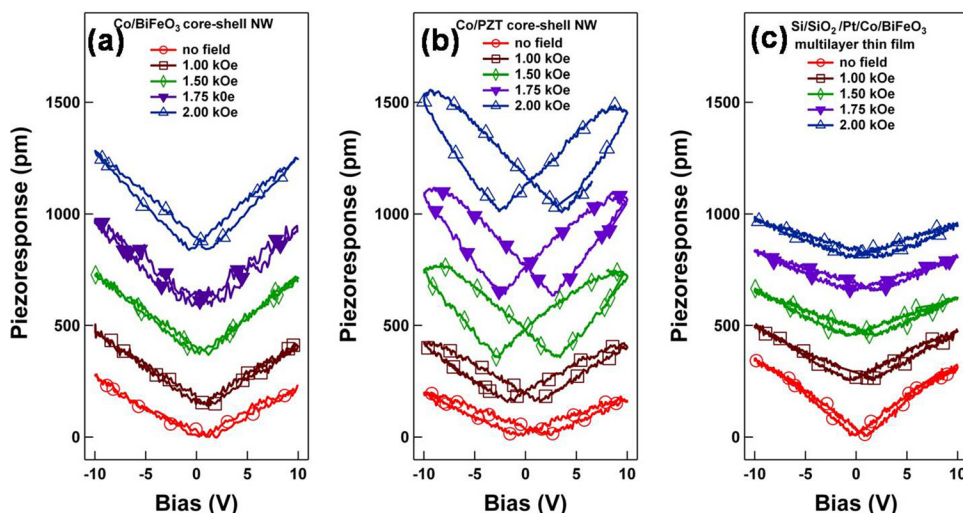


FIG. 2. (Color online) Piezoresponse amplitude, plotted as functions of voltage applied across the BiFeO₃ shell, at selected values of applied magnetic field H , as denoted in the legend, for (a) a Co-core, BiFeO₃-shell NW for $H \perp z$; (b) a Co-core, PbZr_{0.52}Ti_{0.48}O₃ NW, also for $H \perp z$; and (c) a planar Co/BiFeO₃ thin film heterostructure with H parallel to the film plane. Traces are offset vertically for clarity.

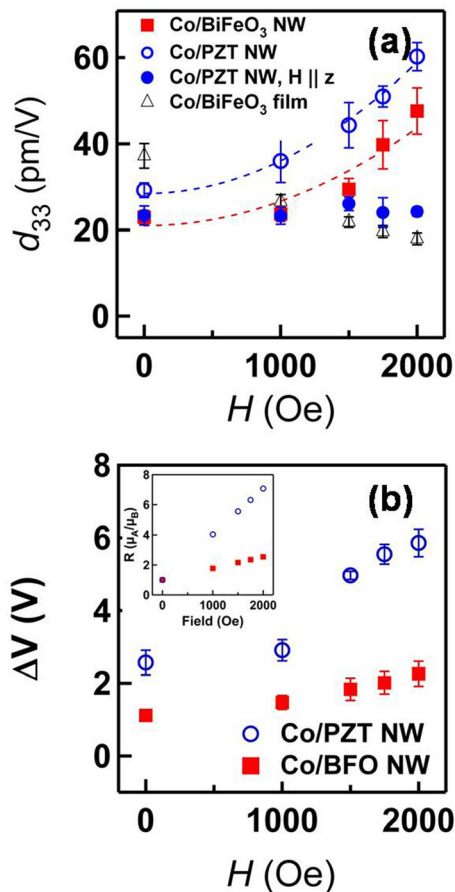


FIG. 3. (Color online) (a) Measured variation in d_{33} with H as obtained from data shown in Fig. 2 and (b) variation in hysteresis loop width with H ; inset: calculated variation in stress intensity ratio $R(=\mu_a/\mu_b)$ with H based on magnetoelastic tuning of ferroelectric coercivity.

free energy formalism to obtain stress-dependence of the FE coercivity, using the renormalized Landau stiffness $\hat{A}(r) = A - 2Q_{11}\sigma_{rr}(r) - 2Q_{12}\sigma_{\phi\phi}$ and other Landau coefficients,¹² with Q_{11} and Q_{12} denoting the electrostriction parameters for BiFeO₃.¹³ Defining μ_a and μ_b as surface tensions at the inner and outer surfaces of the shell of inner and outer radii a and b , respectively, and shell boundary conditions $\sigma_{rr,b} = \mu_b/b$ (tensile) and $-\sigma_{rr,a} = \mu_a/a$ (compressive) we identify, using nonlinear regression, a set of mechanical boundary condition values $\sigma_{rr,a}$ that satisfy our observed relative changes in ΔV with H (inset, Fig. 3(b)). Specifically, loop widths were calculated for BiFeO₃ and PZT by iteratively solving the LG equation with an increasing electric field term starting with positive and negative initial states; the loop width was taken as the value of the electric field term where both the solution was independent of the sign of the initial solution. The loop width was then calculated as a function of the stress at the internal surface of the shell. The electric field units were treated as arbitrary: the calculated

loop widths are normalized to the equilibrium case (same stress on inner and outer surfaces). Within this simple model, this analysis permits us to map H to FE coercivity. Here, we express the strength of the variation of magnetoelastic stress at the core-shell interface with H in the form of a magnitude of stress ratio $R(H)(=\mu_a/\mu_b)$ (Fig. 3(b)): within this model, the change in FE coercivity at 2 kOe can be related to a stress intensification (R) of ~ 7 (~ 2) times that of the field-free case for the Co/PZT (Co/BFO) NW.

Despite consisting of components having characteristic sizes (diameter, shell thickness) smaller than magnetic and dipolar correlation lengths, these results demonstrate how a composite nanostructure can be arranged in a form to produce a significant ME response as evinced by a magnetic field-induced coupling to the converse piezoelectric coefficient. This magneto-elastic response for this FM-FE nanostructure is aided by extreme curvature of the FE shell, the geometric dominance of the interface as a fraction of the total volume of the NW, and magnetic shape anisotropy of the FM nanowire core. In addition to its utility as a nanostructured sensor of magnetic field and its relevance for broadening the selection of ferroelectrics to include Pb-free materials, we anticipate that these results will generate interest in seeking further understanding of ME coupling in nano-scale materials.

The authors thank Brian Beatty, Guannan Chen, and Eric Gallo for assistance with materials characterization, device fabrication, and thin-film sample preparation. Work at Drexel was supported by the ARO (W911NF-08-1-0067) and in part by the ONR (N00014-1-11-0370). P.F. also acknowledges ONR for full support of this work.

- ¹C. W. Nan, M. I. Bichurin, S. Dong, and D. Viehland, *J. Appl. Phys.* **103**, 031101 (2008).
- ²M. Fiebig, *J. Phys. D: Appl. Phys.* **38**, R123 (2005).
- ³N. A. Spaldin, *Magnetic Materials: Fundamentals and Device Applications* (Cambridge Press, Cambridge, 2003).
- ⁴H. Zheng, J. Wang, S. E. Lofland, Z. Ma, L. Mohaddes-Ardabili, T. Zhao, L. Salamanca-Riba, S. R. Shinde, S. B. Ogale, F. Bai, D. Viehland, Y. Jia, D. G. Schlom, M. Wuttig, A. Roytburd, and R. Ramesh, *Science* **303**, 661 (2004).
- ⁵M. D. Glinchuk, E. A. Eliseev, A. M. Morozovska, and R. Blinc, *Phys. Rev. B* **77**, 024106 (2008).
- ⁶S. S. Nonnenmann, E. M. Gallo, M. T. Coster, G. R. Soja, C. L. Johnson, R. S. Joseph, and J. E. Spanier, *Appl. Phys. Lett.* **95**, 232903 (2009).
- ⁷S. S. Nonnenmann, O. D. Leaffer, E. M. Gallo, M. T. Coster, and J. E. Spanier, *Nano Lett.* **10**, 542 (2010).
- ⁸N. B. Chauré, P. Stamenov, F. M. F. Rhen, and J. M. D. Coey, *J. Magn. Mater.* **290**, 1210 (2005).
- ⁹S. Ezhilvalavan and V. D. Samper, *Appl. Phys. Lett.* **86**, 072901 (2005).
- ¹⁰R. M. Bozorth, *Ferromagnetism* (Wiley, Hoboken, NJ, 1993).
- ¹¹H. Schlörb, V. Haehnel, M. S. Khatri, A. Srivastav, A. Kumar, L. Schultz, and S. Fahler, *Phys. Status Solidi* **247**, 2364 (2010).
- ¹²A. M. Morozovska, E. A. Eliseev, S. V. Svechnikov, A. D. Krutov, V. Y. Shur, A. Y. Borisevich, P. Maksymovych, and S. V. Kalinin, *Phys. Rev. B* **81**, 205308 (2010).
- ¹³G. Catalan and J. F. Scott, *Adv. Mater.* **21**, 2463 (2009).